# Heat treatment–microstructure–mechanical/tribological property relationships in austempered ductile iron

T. Nasir[1], D. O. Northwood[1], J. Han[2], Q. Zou[2], G. Barber[2], X. Sun[3] & P. Seaton[3]
*[1]Mechanical, Automotive and Materials Engineering,*
*University of Windsor, Canada*
*[2]Mechanical Engineering, Oakland University, USA*
*[3]Chrysler LLC Tech Center, USA*

## Abstract

Austempered Ductile Iron (ADI) can offer an excellent combination of low cost, design flexibility, good machinability, high strength-to-weight ratio, good toughness, good wear resistance and fatigue strength. Although ADI has found quite wide application in some industries, its use in automotive parts production has been limited. The properties of ADI can be tailored by changing the heat treatment schedule. In this research a Ni-Cu-Mo ADI was subjected to heat treatment schedules involving various austenitizing and austempering process times and temperatures. The mechanical (hardness, toughness) and tribological (scuffing) properties were determined and they were related to both the microstructures and the heat treatment procedures. The highest scuffing resistance is obtained in ADI with a feathery ausferrite microstructure. Such a microstructure also produces the highest toughness but hardness values are only at the Grade I or II levels.

*Keywords: austempered ductile iron, microstructure, hardness, toughness, scuffing, plastic deformation.*

## 1 Introduction

Austempered ductile iron (ADI) has recently appeared as an important engineering material owing to its exceptional combination of high strength,

ductility, toughness, machinability and wear and fatigue resistance. ADI's high strength and toughness, together with its castability, has made it a potential substitute for forged/wrought steel and their assembly-oriented fabrication methods.

The excellent properties of ADI are related to its unique ausferrite microstructure that consists of ferrite and high-carbon stable austenite [1–4]. This microstructure is produced through a 2-step heat treatment process. Step 1 is austenitizing in the temperature range of 850-950°C. Step 2 is to quench to an austempering temperature of 250-400°C and hold for a controlled time period, and then finally cool to room temperature [1]. During the austempering process, austenite undergoes 2 phase transformations. In phase transformation 1, austenite ($\gamma$) transforms into bainitic ferrite ($\alpha$) and high-carbon retained austenite ($\gamma_{hc}$), and in phase transformation 2, the carbon enriched austenite ($\gamma_{hc}$), further decomposes into ferrite and carbide ($\varepsilon$) [2]. The transformations of the two phases are shown in Equations (1) and (2).

$$\text{Phase transformation 1:} \quad \gamma \rightarrow \alpha + \gamma_{hc} \tag{1}$$
$$\text{Phase transformation 2:} \quad \gamma_{hc} \rightarrow \alpha + \varepsilon \tag{2}$$
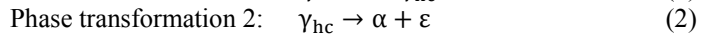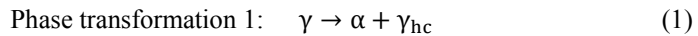
A significant number of studies have been carried out on the tribological behavior of ADI [5–8], but few studies have examined scuffing. Magalhães and Seabra [9] found that heat treating to produce a material that is simultaneously strong and ductile, helps resist scuffing. However there is limited published research on the effect of heat treatment on the microstructure, mechanical and tribological property relationships. The present research examines the effect of heat treatment schedules on the microstructure, hardness, toughness and the scuffing properties of a Ni-Cu-Mo ADI alloy and develops microstructure-property relationships.

## 2  Experimental details

The ADI composition used was (wt%): 1.61 Ni, 0.11 Mo, 0.78 Cu, 3.76 C, 0.24 Mn, 2.51 Si, 0.057 Mg, and traces of S and P. ADI samples were austenitized in a salt bath at 890°C for 20min, and austempered in another salt bath at temperatures of 275°C, 300°C, 325°C, 350°C, or 375°C for times of 10min, 60min, or 150min.

An X-ray diffraction (XRD) method with Cr-K$\alpha$ radiation ($\lambda$=2.29 Å at 20 kV and 20 mA), was used to determine the volume fraction of retained austenite by the direct comparison method using the integrated intensities of the (200)$\alpha$ and (211)$\alpha$ peaks of ferrite, and the (200)$\gamma$ and (220)$\gamma$ peaks of austenite [10].

Charpy impact tests were performed according to the ASTM E23 Standard to evaluate toughness. The tests were carried out on V-notched 55mmX10mmX10mm samples. The impact velocity was 17.21 ft/s. Three tests were conducted for each heat treatment condition, and the average value is reported in this paper. Rockwell hardness tests were conducted on each of the Charpy samples with a 150Kg load (C Scale). A total of 5 readings were taken

for each sample and, the average value is reported in this paper. All tests were conducted at ambient temperature.

A ball-on-disc tribometer was used for the scuffing tests. The ball sample was made of 52100 steel with a diameter of 0.3125mm and a hardness of 66 HRC. The ADI disc samples had a diameter of 75mm and a thickness of10mm. The interface was lubricated by white mineral oil with a viscosity of 33.5cSt at 40ºC. The linear sliding speeds were 1.649 m/s or 1.356m/s. The applied normal load was increased 22N every 120 seconds. Failure load was recorded when there was an abrupt rise in the friction coefficient, noise and vibration. All tests were repeated 4 times and the average coefficient of friction (COF) and scuffing load were recorded. Scuffed samples were then cross sectioned and observed using SEM metallography.

## 3   Results and discussion

### 3.1  Microstructures

The 'as-cast' sample (Fig. 1a) is predominantly pearlitic (85%) ductile iron, with ferrite and nodular graphite. The bright ferrite regions surrounding the dark graphite nodules often are termed as '*Cow's Eye*'. In the austempered samples, the pearlite-ferrite microstructure changes to ausferrite, martensite and retained austenite phases. 3 types of microstructures are observed. At lower austempering temperatures (275, 300°C) it was mostly martensite (Fig. 1b), with a smaller amount of retained austenite (12-28%: values from XRD given in Table 1). At high austempering temperatures (350, 375°C) it was ausferrite (Fig. 1c) with larger areas of retained austenite (27-36%). An intermediate temperature (325°C) had a mixed ausferrite-martensite microstructure (Fig 1d), where the martensite needles were distributed in ausferrite. The retained austenite zones were in form of '*dried-rivers*', with small carbide '*islands*' ($Fe_3C$) particles forming inside. Alloying elements such as Si, Ni, Mo, Cu help retain the carbon-enriched retained austenite and avoid pearlite formation during austempering. Austenite formed in the austenitizing stage transforms into martensite, ausferrite or stable austenite depending on the austempering time/temperature. The higher temperature and longer time samples had more austenite, as the prolonged time allows carbon diffusion to transform austenite into high carbon retained austenite and bainitic ferrite, which is the phase-1 of the transformation. Longer austempering period also allows phase-2 transformation where the high carbon retained austenite further breaks into ferrite and emrbittling cementite ($Fe_3C$), which are termed as '*carbide islands*' in this paper. One of the main purposes of the alloying elements is to avoid the carbide formation during austenitization [2, 4].

The austempering time also had noticeable effect in the microstructure. The martensitic samples had coarse needles in 10min and 150min samples, and relatively fine needles in 60min samples. In ausferritic samples, the ausferrite was mostly feathery for longer austempering times (60-150min) and less feathery for short austempering time (10min). Also 150 min samples had more

carbide particles in the retained austenite rivers. Figs 2a and b compare the medium (325°C, 10min) and highly (350°C, 60min) feathery ausferrite microstructures.
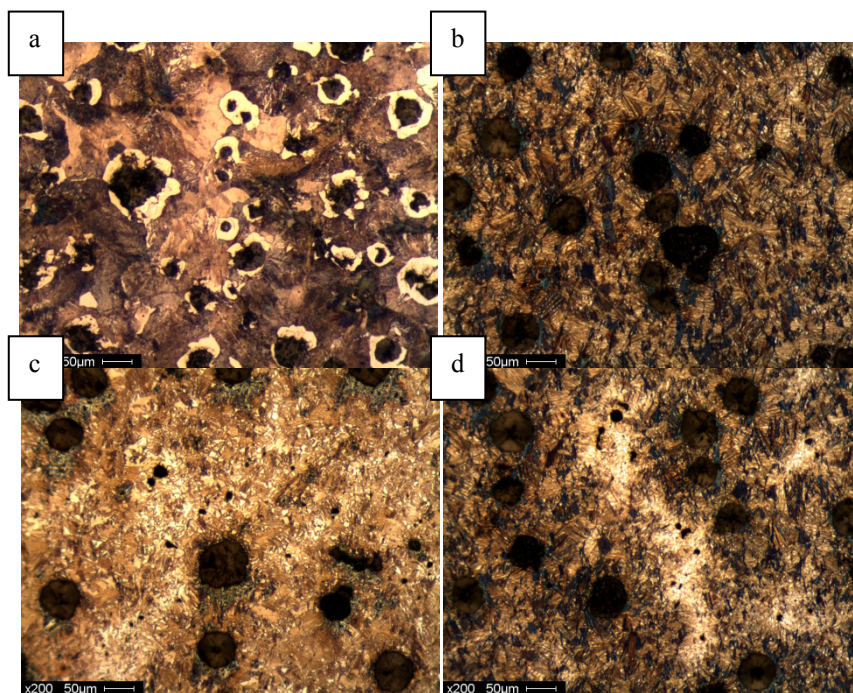


Figure 1:    Optical micrographs of (a) As-cast sample; (b) 10min at 275°C; (c) 60min at 350°C; (d) 60 min at 325°C.
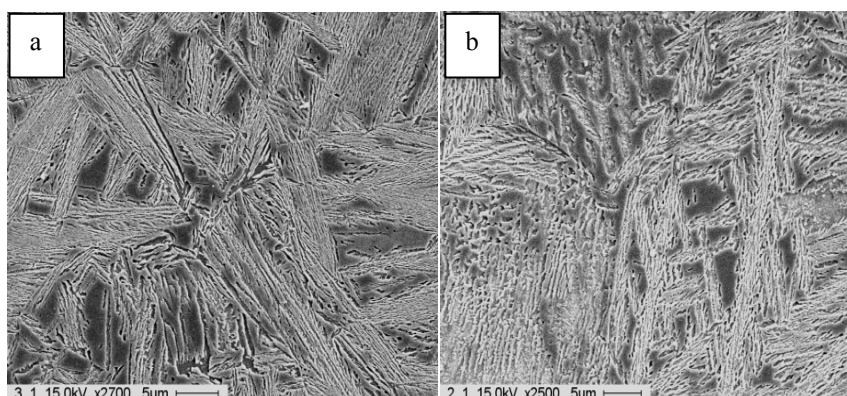


Figure 2:    SEM micrographs of: (a) Medium feathery ausferrite; (b): Highly feathery ausferrite.

## 3.2  Mechanical properties

The combined test results for the different austempering schedules are presented in Table 1. The color coding (white, medium gray and dark-gray) is used to show the lower, median and higher values of the various parameters.

Table 1:    Summary of % retained austenite, mechanical and tribological properties of ADI austempered for different times/temperatures.

| Austempering Temperature (C°) | Time (Mins) | Retained Austenite (vol %) | Hardness (HRC) | Charpy (J) | Scuffing Load1.65 (m/s) | Scuffing Load1.35 (m/s) | |
|---|---|---|---|---|---|---|---|
| As-cast | 0 | 0 | 23 | 2.2 | - | - | |
| 275 | 10 | 12 | 55.8 | - | 90 | 150 | |
| | 60 | 15 | 46 | 4.11 | 103 | 140 | |
| | 150 | 14 | 45.1 | 4.36 | 118 | 148 | |
| 300 | 10 | 18 | 51 | - | 108 | 136 | Low |
| | 60 | 28 | 42.1 | 5.13 | 124 | 145 | |
| | 150 | 27 | 42.4 | 5.46 | 110 | 150 | |
| 325 | 10 | 23 | 45.7 | - | 118 | 155 | Med |
| | 60 | 33 | 35.2 | 5.96 | 170 | 170 | |
| | 150 | 33 | 36.7 | 6.28 | 126 | 162 | |
| 350 | 10 | 27 | 45.4 | - | 124 | 155 | High |
| | 60 | 35 | 32 | 5.98 | 170 | 178 | |
| | 150 | 34 | 32 | 6.71 | 140 | 140 | |
| 375 | 10 | 29 | 45.2 | - | 128 | 165 | |
| | 60 | 36 | 27.6 | 6.45 | 177 | 185 | |
| | 150 | 35 | 27.6 | 9.20 | 143 | 182 | |

A low austempering temperature and short time give a high hardness value, with the highest hardness of HRC 55.8 for 275°C/10min (Table 1). This is due to the martensitic microstructure, and low % retained austenite. Hardness decreases with increasing austempering temperature and time: the lowest hardness of HRC 27.6 is achieved at 375°C/60 min and 150 min. All five principal hardness grades (I-V) of ADI [11] can be developed by choice of austempering temperature and time, and the hardness is significantly higher than the as-cast sample. In Table 1, the "low" coding for hardness values corresponds to Grades I and II, the "Median" coding to Grades III and IV, and the "High" coding to Grade V. Hardness decreases with increasing % retained austenite, which reflects the amount of ausferrite which is significantly softer than the martensitic microstructure. Figure 3 and Equation (3) show the inverse relationship between % retained austenite (RA) and hardness (H):

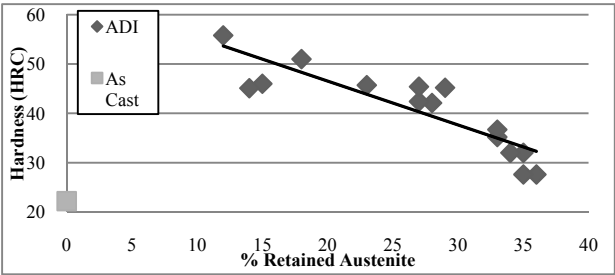$$H = -0.8889(RA) + 64.298 \quad (R2 = 0.7687) \qquad (3)$$

Figure 3:    The relationship between % retained austenite and hardness.

It should be emphasized that the Charpy results in Table 1 are for notched samples and, as such, are much lower values than reported for un-notched samples [12]. From Table 1 and Fig 4a, we can see that ADI samples with higher % retained austenite exhibit higher toughness. These results for toughness agree with previous work on alloyed ADI where fracture toughness reached a maximum for retained austenite contents around 30% [13]. Consequently, longer austempering times (60-150 mins) give higher toughness values. A feathery ausferrite microstructure thus provides a higher toughness. A martensitic structure (275-300°C) gives the lowest toughness. All heat-treated samples had a higher toughness than the as-cast sample (2.2J) and Figs 4a and b show that the toughness is proportional to % retained austenite and inversely proportional to the hardness. The SEM fractographs of the as-cast and highest toughness samples are shown in Figs 5a and b. Fractographic observation shows the existence of river patterns and cleavage facets in the as-cast sample: see Fig. 5a. A more ductile fracture with micro cup and cone features is seen in the samples with a feathery ausferrite structure: see Fig. 5b.
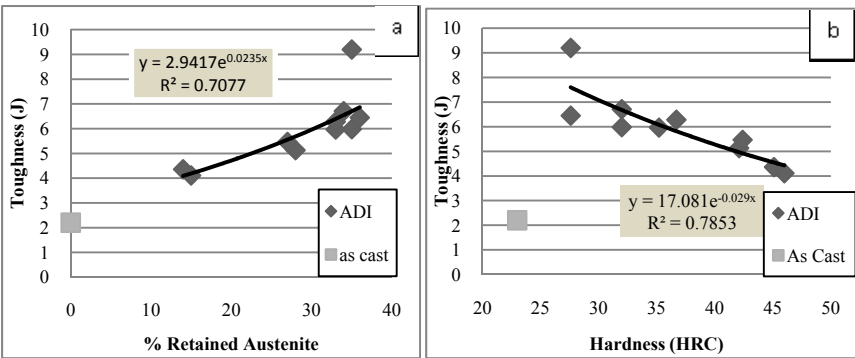


Figure 4:    Relationship between toughness and (a) % retained austenite and (b) hardness.
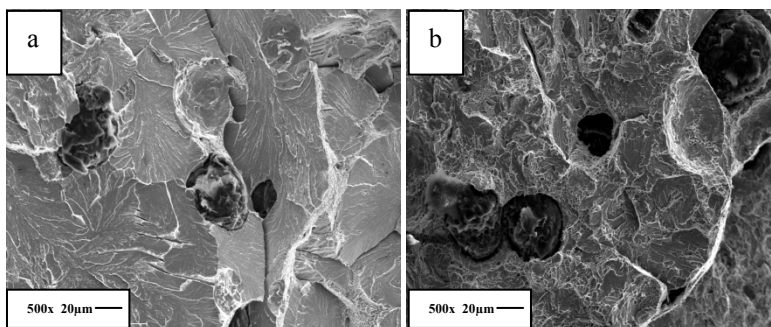
Figure 5:    SEM fractographs of Charpy samples (a) as–cast (lowest toughness). (b) 375°C, 150 min (highest toughness).

## 3.3  Scuffing performance

The relationship between the scuffing load (L) and hardness (H), % retained austenite (RA), and toughness (C) for both speeds are presented in Figs 6a–c, and Equations (4)–(9).

$$L = 138 - 4.496RA + 0.144(RA)^2 \quad (R^2=0.749; 1.649 \text{ m/s}) \qquad (4)$$
$$L = 138 - 4.496RA + 0.110(RA)^2 \quad (R^2=0.586; 1.356 \text{ m/s}) \qquad (5)$$
$$L = 235 - 2.561H - 0.0H^2 \qquad (R^2=0.728; 1.649\text{m/s}) \qquad (6)$$
$$L = 294.6 - 5.685H - 0.054H^2 \quad (R^2=0.540; 1.356 \text{ m/s}) \qquad (7)$$
$$L = -6.36C^2 + 93.13C - 175.18 \qquad (R^2= 0.6052; 1.649 \text{ m/s}) \qquad (8)$$
$$L = -1.3C^2 + 25C + 59.88 \qquad (R^2= 0.4388; 1.356\text{m/s}) \qquad (9)$$

It can be seen from Table 1 that for both speeds the scuffing load is higher for medium and high austempering times and temperatures. The scuffing load increases with the % retained austenite: see Fig. 6a. The polynomial curve fitting gives an acceptable coefficient of determination $R^2$ values in Equations (4) and (5). For both sliding speeds, scuffing load increases with decreasing hardness: see Fig. 6b and Equations (6) and (7). As hardness is inversely proportional to toughness, the scuffing load increases with higher Charpy values as shown in Fig. 6c. The range for toughness is approximately 5.5 to 7 J, where the scuffing load was found to be highest. For the same notched sample, the as-cast sample had a toughness of 2.16J. Polynomial curve fitting provided a relationship between scuffing load (L) and toughness (C): see Equations (8) and (9). The scuffing load decreases with an increase of sliding speed. The higher speed data (1.649 m/s) has higher $R^2$ values compared to the lower speed (1.356 m/s) in all the plots (Figs 6(a-c)). This suggests that scuffing resistance at the higher sliding speed is less predictable. The maximum scuffing loads were found for samples with a higher fraction of feathery ausferrite (375°C, 60min-176N), and samples with a smaller amount of ausferrite and higher martensite content showed lower scuffing loads (275°C, 10min-88N). Thus it can be deduced that the martensite-ausferrite balance in the microstructure is important in the scuffing performance.
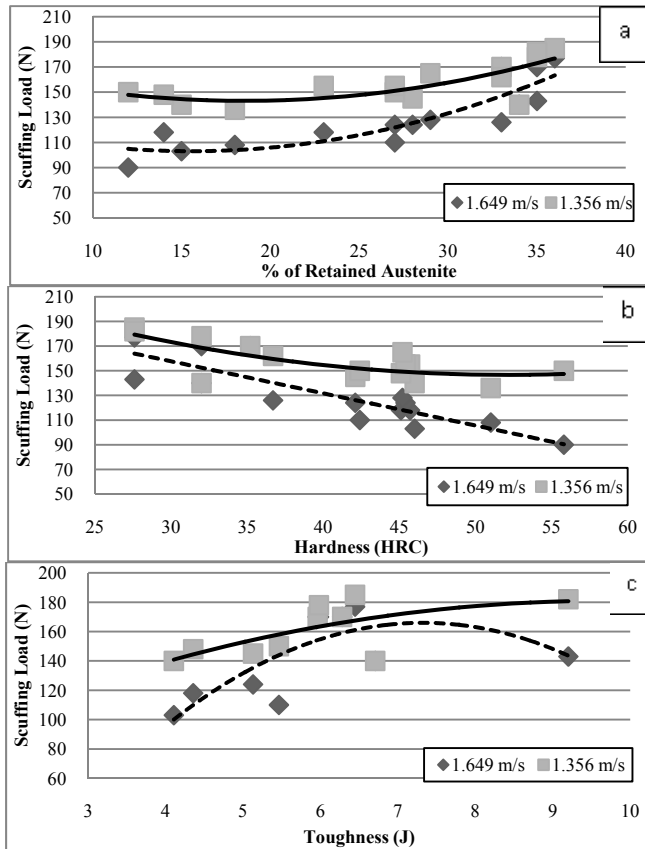
Figure 6:     Relationship between scuffing load and (a) % retained austenite, (b) hardness and (c) toughness.

## 3.4  Metallurgical examination of scuffed samples

Figures 7 (a–i) show the cross-sectional views of the scuffed track of the ADI samples. Figures 7 (a-c) are samples with an austempering time of 10min. Cracks are observed at the graphite/martensite matrix interfacial regions in the subsurface and cracks are seen to be propagating from the interfacial regions. The result of this crack propagation will be the generation of a wear particle and the "pull-out" of graphite. Shelton and Bonner [14] in their study of copper-containing ADI also suggested that sub-surface crack initiation and propagation, which lead to the surface delamination, always initiated at the graphite nodules. An in-situ observation of the microprocess of crack initiation and propagation in ADI by Dai et al. [15] also gave similar findings. Very little plastic deformation was observed on most samples except for the sample austempered at 375°C for 10 minutes (Fig. 7c) which has the highest content of ausferrite for samples

austempered for 10 minutes (Table 1). Moderate plastic deformation was observed for the scuffed samples which were austempered at temperatures of 275ºC and 300°C for 60min and 150min: see Figs 7 (d-f). A few cracks were also observed, which are expected to produce wear particles after propagation. There was also deformation of the graphite due to the scuffing process. A large amount of plastic deformation was found in the ausferrite matrix with high austempering temperatures of 350°C and 375°C at 60min; Figs 7 (h-i).

Cracks can initiate easily in the harder surface during the sliding contact. Macrostructures with a hard martensitic matrix cannot "protect" the graphite nodules. The graphite is prone to pull out during sliding because of its weak strength; consequently, cracks can be propagated as in Figs 7 (a-c). After a low critical number of cycles, a large amount of wear particles are produced. These
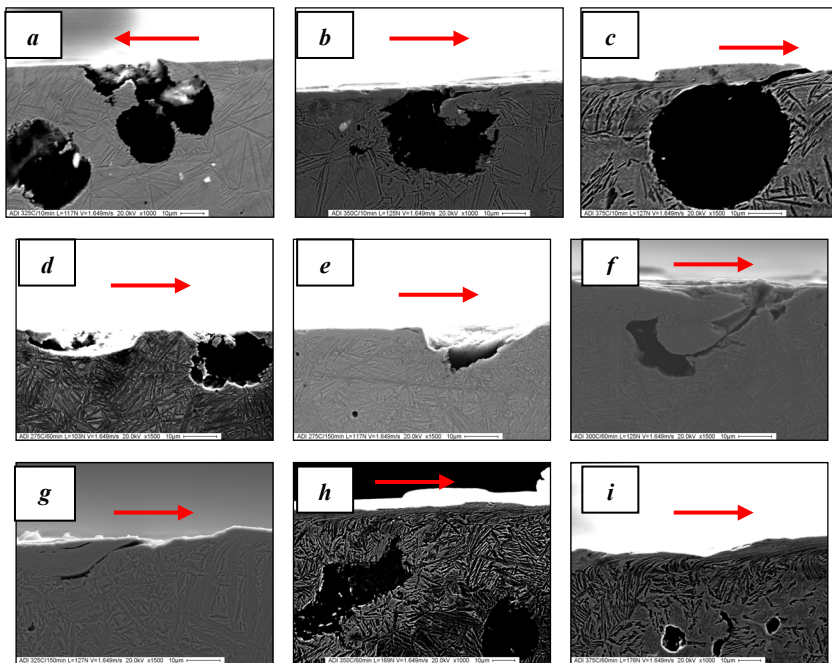


Figure 7:    SEM image in the subsurface micrograph at sliding speed of 1.649m/s (the horizontal arrow shows the sliding direction) for ADI austempered in (a) 325ºC/10min, scuffing load=117N; (b) 350ºC/10min, scuffing load=125N; (c) 375ºC/10min, scuffing load=127N; (d) 275ºC/60min, scuffing load=103N; (e) 275ºC/150min, scuffing load=117N; (f) 300ºC/60min, scuffing load=125N; (g) 325ºC/150min, scuffing load=127N; (h) 350ºC/60min, scuffing load=169N; (i) 375ºC/60min, scuffing load=176N.

particles destroy the lubricant film, leading to metal-to-metal contact and eventually, catastrophic failure. This leads to a low scuffing resistance. This theory is also supported by the scuffing load-toughness relationship. Scuffing load is inversely proportional to the toughness. Samples with lower toughness would be prone to surface cracks and debris accumulation, leading to lubricant film destruction. A tougher surface is thus the key to an improved scuffing performance.

A trace of a white layer is observed in the Fig. 7g. This "white layer" constituent has been mentioned in cast iron research studies dating back to 1940s. Clayton and Jenkins [16] found that a cast iron surface rubbing against steel develops a thin layer of a white constituent. The material was assumed to have two phases; cementite and a high carbon ferritic base developed from austenite. Ludema [17] in his research on scuffing for a lubricated surface mentioned of the formation of a white layer. This white layer is termed as W2. XRD and transmission electron microscopy (TEM) analysis by Cranshaw and Campany [18] suggested that W2 was a heavily deformed mixture of austenite and martensite. The formation of the strain induced martensite in austempered ductile iron has been discussed in detail by Daber and Rao [19] and Daber et al. [20]. The transformation of austenite to martensite on the surface has been shown by both Johansson [21] and Ball et al. [22] to lead to an increase in wear resistance of austenitic-bainitic ductile iron and stainless steels.

## 4   Conclusions

This study on the effect of austempering heat treatment schedule (temperatures from 275-375°C at times from 10 to 150 minutes) has shown that the highest scuffing resistance of an Ni-Cu-Mo ADI alloy is obtained with samples exhibiting a feathery ausferrite microstructure (also termed upper ausferrite) obtained at 375°C or 350°Cfor 60/150 mins. Such a microstructure, which contains about 30% retained austenite, gives the highest toughness values but hardness values only at the Grade I or II levels.

Austempering at lower temperatures (275–325°C) or shorter times lead to a partial martensitic structure, lower levels of retained austenite, higher hardness levels (Grade III to V), lower toughness and poorer scuffing performance which is attributed to cracking initiated at the graphite nodule-martensite interface, resulting in the generation of wear particles.

## References

[1]  Bosnjak, B., Radulovic, B., Effect of austenitising temperature on austempering kinetics of Ni-Mo alloyed ductile iron. *Materiali in Tehnologije,* **38 (6),** pp 307-312, 2004.
[2]  Yang, J., Putatunda, S. K., Improvement in strength and toughness of austempered ductile cast iron by a novel two-step austempering process. *Materials and Design,* **25***,* pp 219–230, 2004.

[3]   Myszka D., Austenite-martensite transformation in austempered ductile iron. *Archives of Metallurgy and Materials,* **52(3)***,* pp475-480, 2007.
[4]   Eric, O., Jovanovic, M., Microstructure and mechanical properties of Cu-Ni-Mo austempered ductile iron. *Journal of Mining and Metallurgy,* **40B (1)** pp 11-19, 2004.
[5]   Sahin, Y., Erdogan, M., Kilicli, V., Wear behaviour of austempered ductile iron with dual matrix structures. *Materials Science and Engineering,* **A444***,* pp31-38, 2007.
[6]   Perez, M. J., Cisneros, M. M., Lopez, H. F., Wear resistance of Cu-Ni-Mo austempered ductile iron. *Wear, 260,* pp 879-885, 2006.
[7]   Kumari, U. R. and Rao, P. P., Study of the wear behaviour of austempered ductile iron. *J. Materials Science*, **44**, pp 1082-1093, 2009.
[8]   Zimba, J., Samandi, M., Yu, D., Chandra, T., Navara, E. And Simbi, D. J., Un-lubricated sliding wear performance of unalloyed austempered ductile iron under high contact stresses. *Materials and Design*, **25**, pp 431-438, 2004.
[9]   Magalhães, L., Seabra, J., Wear and scuffing of austempered ductile iron gears. *Wear,* **215**, pp237-246, 1998.
[10] ASTM Standard (E975-03), Standard practice for X-Ray determination of retained austenite in steel with near random crystallographic orientation. American Society for Testing and Materials, ASTM International: West Conshohocken, PA, USA, 2003.
[11]  Properties and selection irons, steels, and high-performance alloys: *Metals Handbook, Vol.1,* 10th edition*,* ATSM International: Materials Park,  OH, USA, 1990.
[12] Trudel, A. And Gragné, M., Effect of composition and heat treatment parameters on the characteristics of austempered ductile irons. *Canadian Metalllurgical Quarterly, 36(5)*, pp 289-298, 1997.
[13] Eric, O., Rajnovic, D., Burzic, Z., Sidjanin, L. and Jovanovic, M., T., Fracture toughness of alloyed austempered ductile iron (ADI): Fracture of Nano and Engineering Materials and Structures. **C23**, pp 1145-1146, 2006.
[14] Shelton, P. W., Bonner, A. A., The effect of copper additions to the mechanical properties of austempered ductile iron (ADI). *Journal of Materials Processing Technology, 173,* pp 269-274, 2006.
[15] Dai, P. Q., He, Z. R., Zheng, C. M., Mao Z. Y., In-situ SEM observation of the fracture of austempered ductile iron. *Material Science and Engineering,* **A319-321**, pp 531-534, 2001.
[16] Clayton, D., Jenkins, C. H. M., Physical changes in rubbing surfaces on scuffing. *British Journal of Applied Physics,* **2**, pp 69-78, 1951.
[17] Ludema K. C., A review of scuffing and running-in of lubricated surfaces, with asperities and oxides in perspective. *Wear,* **100**, pp315-33, 1984.
[18] Cranshaw, T. E., Campany, R. G., The study of scoring and scuffing on lubricated sliding surfaces by Mossbauer spectrography. *Journal De Physique,* **C2**, pp 589-591, 1979.

[19] Daber, S., Rao, P., P., Formation of strain-induced martensite in austempered ductile iron. *Journal of Material Science,* **43,** pp 357-375, 2008.

[20] Daber, S., Ravishankar, K., S., Rao, P., P., Influence of austenitizing temperature on the formation of strain induced martensite in austempered ductile iron. *Journal of Material Science,* **43,** pp 4929-4937, 2008.

[21] Johansson, M., Austenitic-bainitic ductile iron. *AFS transactions,* **85**, pp 117-122, 1977.

[22] Ball, A., Allen, C., Prothoreo, B., The abrasive-corrosive wear of stainless steel. *Wear,* **74**, pp 287-305, 1981.